

Improvement of Spiking Neural Network with Bit Planes and Color Models

Nhan T. Luu*, Duong T. Luu[†], Pham Ngoc Nam[‡], Truong Cong Thang*

* *Department of Computer Science and Engineering, The University of Aizu, Aizuwakamatsu, Japan*

[†] *Information and Network Management Center, Can Tho University, Can Tho, Vietnam*

[‡] *College of Engineering and Computer Science, VinUniversity, Hanoi, Vietnam*

(ltnhan0902@gmail.com, luutd@ctu.edu.vn, nam.pn@vinuni.edu.vn thang@u-aizu.ac.jp)

Abstract—Spiking neural network (SNN) has emerged as a promising paradigm in computational neuroscience and artificial intelligence, offering advantages such as low energy consumption and small memory footprint. However, their practical adoption is constrained by several challenges, prominently among them being performance optimization. In this study, we present a novel approach to enhance the performance of SNN for images through a new coding method that exploits bit plane representation. Our proposed technique is designed to improve the accuracy of SNN without increasing model size. Also, we investigate the impacts of color models of the proposed coding process. Through extensive experimental validation, we demonstrate the effectiveness of our coding strategy in achieving performance gain across multiple datasets. To the best of our knowledge, this is the first research that considers bit planes and color models in the context of SNN. By leveraging the unique characteristics of bit planes, we hope to unlock new potentials in SNNs performance, potentially paving the way for more efficient and effective SNNs models in future researches and applications.

Index Terms—Spiking neural network, spike coding, image classification

I. INTRODUCTION

The field of artificial intelligence (AI) has experienced unprecedented advancements in recent decades [1], largely driven by the developments of deep learning algorithms. Despite these advancements, traditional artificial neural networks (ANNs) often fall short in modeling the intricate and dynamic nature of biological neural systems [2]. To bridge this gap, spiking neural networks (SNNs) have emerged as a promising alternative, leveraging the temporal dimension of neuronal activity to more closely emulate the behavior of biological brains.

SNNs utilize discrete spike events to transmit information between neurons, mirroring the asynchronous and event-driven communication observed in biological neurons [3]. This approach not only enhances the biological plausibility of neural models but also offers potential advantages in terms of computational efficiency and power consumption, particularly for hardware implementations [4]. The inherent sparsity and temporal coding of SNNs provide a robust framework for developing low-power neuromorphic systems that can operate efficiently in real-time environments [5].

Despite their potential, SNNs pose significant challenges, particularly in training methodologies and network optimization. Traditional backpropagation techniques used in ANNs are not directly applicable to SNNs due to their discontinuous and non-differentiable nature [6]. Consequently, novel training algorithms, such as spike-timing-dependent plasticity (STDP) [7], [8] and surrogate gradient methods [9], have been developed to address these challenges, enabling the effective training of SNNs.

Prior research in ANN has explored the application of bit planes (e.g. [10]) and color models [11], [12] to enhance performance across various tasks, demonstrating significant improvements in areas such as image recognition and processing. Motivated by these advancements, we aim to investigate whether bit planes and color models can similarly improve the performance of SNNs. This led us to formulate our research questions:

- *Does bit plane representation enhance the performance of SNN?*
- *What are impacts of different color models on SNN?*

Especially, we observe that bit planes of an image contain pulse-like information, and can be applied to encode color information for SNNs to possibly improve accuracy. After extensive experimentation, we concluded that bit planes contain valuable information that can be utilized in the rate coding process as a supplementary source to enhance the accuracy of direct surrogate backpropagation process [13] in SNN architectures. Furthermore, bit plane information proved to be reusable across multiple color models in most of the cases examined in our study.

A preliminary version of this paper is published in [14], where the benefit of including bit plane coding is proved by three grayscale datasets. In this extended version, the following new points have been added. First, the proposed method was updated to support color images. Second, eight more datasets are included. Third, impacts of color models are investigated.

II. SPIKING NEURAL NETWORK

In this section we present an overview of SNN knowledge related to our research.

A. History of SNNs

Phenomenological neuron models can be progressively simplified until reaching a stage where even neural spikes are not modeled, leading to first and second generation neurons [15], [16]. This simplification significantly reduces computational demands but also decreases biological realism. The detail level in modeling often correlates with available computing power. For example, ANNs based on second generation neurons were historically limited by computing power [17], restricting the size of networks and the complexity of neuronal models. This limitation influenced the design of learning algorithms. Even with advancements in computing power, the complexity of neuronal models did not proportionately increase because existing learning algorithms were not compatible with more detailed models. Consequently, two distinct research fields emerged.

- ANNs [18] focused on large networks of simplified neuron-like units, capable of learning through algorithms like backpropagation, and were successfully applied in pattern recognition, classification, and pattern completion tasks.
- *Computational Neuroscience* [19] in contrast used detailed biophysical and phenomenological models in smaller networks to study electrophysiological processes, pattern generation, and dynamic behaviors of small neuron groups.

Although there have been attempts to create large networks of detailed biophysical neuron models [20], it remains challenging due to computational constraints.

Recent advances in computing power have blurred the lines between these fields. ANNs have become more biologically realistic, while networks of biophysical neurons have grown larger and more detailed. However, computational power still limits the application of detailed models in large neural networks for pattern recognition and classification. With improved computing power, new learning algorithms are being developed for these models. SNNs, which use spiking neurons modeled by phenomenological models like the Spike Response Model [21], represent the next step towards this goal. Due to the computational burden, biophysical models are less common in certain SNN applications. This paper focuses on research involving SNNs with phenomenological models, excluding those using biophysical models.

B. The Integrate-and-Fire model

One of the earliest neuron models is the perfect integrate-and-fire (IF) model (also sometimes referred to as the non-leaky integrate-and-fire model), first studied by Louis Lapicque in 1907 [22]. In this model, the neuron is characterized by its membrane potential V :

$$C \frac{dV(t)}{dt} = I(t) \quad (1)$$

which evolves over time in response to an input current $I(t)$. This evolution is described by the time derivative of the capacitance law, $Q = CV$, where C is the membrane capacitance. As an input current is applied, the membrane potential increases until it reaches a fixed threshold V_{th} . At this point, the neuron generates a spike modeled as a delta function, and the membrane potential is reset to its resting value, after which the process repeats. In this model, the firing rate increases linearly and indefinitely with the increase in input current.

While previous efforts have successfully converted ANN neurons with ReLU activations to IF neurons, challenges still remain in the conversion process. One of the key issues is the difficulty in precisely determining the appropriate thresholds in these conversion approaches. Despite the introduction of both data-driven and model-driven threshold determination methods [23], the converted SNN often experience unstable accuracy compared to their re-trained ANN counterparts. Additionally, IF neurons lack time-dependent memory. Once a neuron receives sub-threshold potentials, the membrane potential persists without decay until the neuron fires. This behavior is said to be inconsistent with biological neurons, which exhibit dynamic temporal properties [24]. Still, within certain SNN architectures, IF neurons have demonstrated superior performance compared to the supposedly better LIF neurons [24], with the SEW-ResNet [25] architecture being one such example.

C. Deep Residual Learning in Spiking Neural Networks

The success of ResNet [27] in deep learning has motivated efforts to extend residual learning to SNN. Prior attempts, commonly referred to as Spiking ResNets [28], have largely replicated the architecture of ResNet [27] by replacing ReLU activation functions with spiking neurons. However, this approach presents certain limitations:

- *Inability to achieve identity mapping across neuron models*: Residual learning is predicated on the concept of identity mapping, where layers can be trained to approximate an identity function. While this is straightforward in ResNets [27] with ReLU activation, it is not always feasible in Spiking ResNets [28]. Specifically, [25] claimed that for certain spiking neuron models, such as leaky integrate-and-fire (LIF) neurons [22] with learnable membrane time constants, ensuring that a spiking neuron fires in response to an input spike becomes challenging. This complicates the realization of identity mapping.
- *Vanishing/exploding gradients*: Even in cases where identity mapping can be achieved, Spiking ResNets [28] are prone to vanishing or exploding gradients during training. This occurs because the gradient propagation through multiple layers of spiking neurons may either diminish to zero or grow uncontrollably, complicating the training of deeper networks.

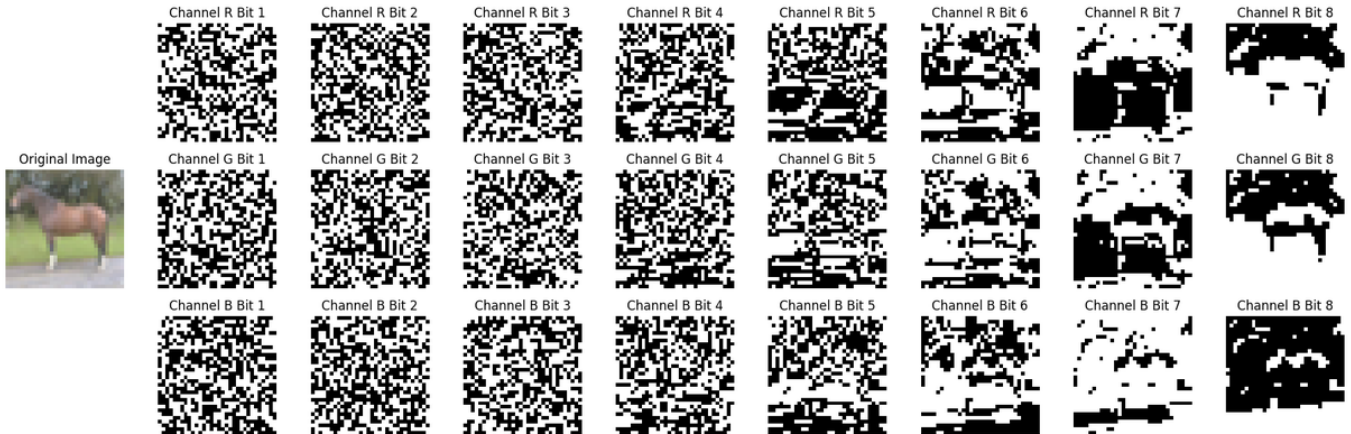


Fig. 1: Illustrated bit planes of a sample image from CIFAR10 [26] dataset.

To address these issues, SEW ResNet [25] was introduced as a replacement design for residual blocks while utilizing IF neurons. The SEW block capitalizes on the binary nature of spikes by applying element-wise functions g to the output of the residual mapping $A_l[t]$ and the input spike train $S_l[t]$ [25]. This approach facilitates identity mapping, mitigates the vanishing/exploding gradient problem and achieves higher accuracy with fewer time steps compared to existing SNN models.

SEW ResNet [25] was also the first work to propose and apply a surrogate gradient approach for optimizing SNNs. Using backpropagation methods to train SNNs [13], [29] has become a common practice in neuromorphic computing. However, applying backpropagation in SNNs presents certain challenges. In SNNs, spike signals are typically modeled using binary values (0s and 1s) from a Heaviside function $H(\theta, t)$, where θ is the membrane potential and t is a threshold:

$$H(\theta, t) = \begin{cases} 1 & \text{if } \theta - t \geq 0 \\ 0 & \text{otherwise} \end{cases} \quad (2)$$

The derivative ∂H of this function is given by:

$$\frac{\partial H}{\partial \theta} = \begin{cases} +\infty & \text{if } \theta - t = 0 \\ 0 & \text{otherwise} \end{cases} \quad (3)$$

As shown, directly differentiating $H(\theta, t)$ results in unstable gradients. To address this, [25] proposed substituting the derivative of the Heaviside function ∂H with a numerically stable gradient from a different activation function during backpropagation, such as the derivative $\partial \sigma$ of the Sigmoid function $\sigma(\theta, t)$:

$$\sigma(\theta, t) = \frac{1}{1 + e^{\theta-t}} \quad (4)$$

$$\frac{\partial H}{\partial \theta} = \frac{\partial \sigma}{\partial \theta} = \frac{e^{\theta-t}}{(e^{\theta-t} + 1)^2}$$

This approach yields a more stable gradient during back-propagation, allowing the use of existing automatic differentiation frameworks to optimize SNNs effectively.

With these advantages, we decided to choose SEW Resnet [25] architecture for our study.

III. BIT PLANES AND COLOR MODELS IN DEEP LEARNING

This section presents an overview of bit planes and color models, along with their applications in deep learning algorithms.

A. Bit planes in deep learning

Bit planes have shown extensive utility in deep learning applications, offering new ways to improve model efficiency and performance. In [10], researchers used bit planes to encode the input layer in Binary Neural Network (BNN). They argued that bit planes retain crucial spatial information, enabling a reduction in the number of multiply-accumulate operations (MACs) without compromising the model's accuracy or robustness. This demonstrates the potential of bit planes in streamlining computations while maintaining competitive performance.

The use of bit plane slicing on RGB images for adversarial robustness was explored in [30]. By selecting the most significant bit planes, the authors developed a classification model that was better equipped to handle adversarial attacks. This approach capitalizes on the spatial information encoded in different bit planes, which helps the model resist manipulations that would otherwise degrade its performance.

In the domain of medical imaging, bit plane slicing has also been applied to improve accuracy in breast cancer recognition tasks [31]. Researchers found that lower-order bit planes are more susceptible to noise, and by removing them before inputting the data into a convolutional neural network (CNN), they achieved higher classification accuracy. This method highlights how bit plane analysis can be tailored to specific

challenges, such as noise reduction in medical images, to enhance model effectiveness.

Although bit planes have been widely studied and applied in ANNs, their utilization in SNNs is still unexplored. As far as we concern, our research is first to explore application of bit planes on SNNs spike coding process.

B. Color models in deep learning

Color models are fundamental in computer graphics as they define how colors are represented, manipulated, and displayed for digital images. In computer graphics applications, understanding and effectively managing color models is crucial for tasks such as rendering realistic scenes, creating digital artwork, and designing user interfaces. Color models can be divided into *device-oriented models*, *user-oriented models* and *device-independent models* [32], [33].

Device-oriented color models are influenced by the signals of the devices and the resulting colors are affected by the technology used for display. Widely utilized in various applications that require color consistency with hardware tools, examples include any hardware devices used for human visual perception, such as televisions and video systems. Popular color models for devices include RGB, CMY(K) and YCbCr.

User-oriented color models are considered as a pathway between the observer and the device handling the color information. For our study, we mostly investigate cylindrically described models, including HSL and HSV. According to [32], these models also inherit other special properties such as device dependence and cylindrical-coordinate representation.

Device-independent color models are essential for defining color signals without reliance on the specific characteristics of any particular device or application. These models play a crucial role in applications that involve color comparisons and the transmission of visual information across networks that connect various hardware platforms. We will mostly research color models defined by the International Commission on Illumination (CIE), including CIE XYZ and CIE LAB.

Color models are becoming increasingly important in deep learning algorithms, offering valuable information that enhances model performance in various tasks. For example, in [34], a research on traffic light recognition tested a range of color models across different deep learning architectures, with results indicating that the RGB model remains favored despite some of its limitations. This suggests that, while RGB is not perfect, it still outperforms other models in certain applications.

In another study on applying convolutional neural networks (CNNs) for skin detection against adversarial attacks of generative models [35], RGB and YCbCr color models demonstrated superior performance, particularly in handling varying lighting conditions. This highlights the adaptability of these color models in scenarios where lighting inconsistencies can degrade model accuracy.

Moreover, the development of ColorNet [11] illustrates the potential of leveraging multiple color models to capture a broader set of features. By combining information from these diverse color models, ColorNet outperforms traditional models that rely on a single color model. However, this approach introduces computational overhead due to the inclusion of smaller submodels, which can be a challenge despite the model's increased efficiency in some cases.

Despite extensive researches on the use of color models in ANN, their application in SNN remains underexplored and requires further investigation.

IV. PROPOSED METHOD

In this section, we present in detail the design of our coding algorithm.

A. Hypothesis and Preliminary Study

We hypothesize that the information contained in the bit planes of an image can be effectively used to encode inputs for SNN training. Bit planes decompose an image into binary levels, each representing a specific bit of the binary representation of pixel values. This decomposition can potentially preserve critical information of the original image while providing a format that might be more suitable for the spike-based processing in SNNs. The granularity of information available in bit planes offers a unique approach to encoding visual data, which could enhance the learning capabilities of SNNs by providing a richer, multi-level representation of the input.

To test this hypothesis, we conducted a preliminary experiment and analysis using the MNIST [36], which is a simple dataset containing gray-scale images of hand-written numbers. For analysis in term of information contained in the coded spike signals, we perform the calculation of the mean base-2 Shannon entropy [37] $\bar{H}(X_j)$ as:

$$\bar{H}(X_j) = -\frac{1}{N} \sum_{j=1}^N \sum_i p(x_i) \log_2 p(x_i) \quad (5)$$

and the approximated average Kolmogorov complexity \bar{K} across all dataset's elements where the Kolmogorov complexity $K(X)$ of a coded image is estimated with DEFLATE compression algorithm [38] $C_{DEFLATE}(X)$ as:

$$\begin{aligned} \bar{K}(X_j) &= \frac{1}{N} \sum_{j=1}^N K(X_j) \\ &\approx \frac{1}{N} \sum_{j=1}^N C_{DEFLATE}(X_j) \\ &= \frac{1}{N} \sum_{j=1}^N Huffman(LZ77(X_j)) \end{aligned} \quad (6)$$

where $Huffman(X)$ is the Huffman coding [39] and $LZ77(X)$ is the LZ77 compression [40] (or sometimes referred to as sliding window compression).

We compared three approaches: traditional spike coding, bit plane coding only, and the combination of both spike coding and bit plane coding. The detailed settings of this experiment can be found in Section V-A. The results are provided in Table I.

Coding method	Validation Accuracy (%)	Averaged Kolmogorov complexity approximation (bits)	Averaged Shannon entropy (bits)
Spike coding	98.62	721.5	0.53
Bit plane coding only	97.87	772.8	0.56
Combination of spike coding and bit plane coding	98.93	744.4	0.55

TABLE I: Average validation accuracy and analysis metrics comparison on MNIST [36]

The results demonstrate that the approximated Kolmogorov complexity and Shannon entropy of bit-plane-coded data are higher, suggesting that the information content is more complex and less predictable. This may help explain why the accuracy of models using exclusively bit-plane-encoded inputs is lower compared to the baseline. On the other hand, a combination of rate coding and bit-plane coding resulted in an increase in performance. This outcome demonstrates that bit planes contain valuable information that SNN can learn from to improve their classification ability. This encourages us to carry out a further study and perform testing on other datasets.

B. Proposed Coding Method with Bit Planes

As we can see in Figure 2, the proposed coding scheme integrates a dual approach featuring both traditional spike coding and bit plane coding methodologies. Initially, the process commences with the conventional spike coding procedure applied to the image tensor. The bit plane coding algorithm (Algorithm 1) is employed to transform an input image into binary planes. The final encoded tensors are then generated through tensor concatenation across the first dimension, merging the outputs from spike coding and bit plane coding. These encoded tensors are thereby prepared for utilization in inference tasks and/or training processes.

Algorithm 1 is designed to encode an image tensor batch X into n_{bit} bit planes. To determine n_{bit} , it is essential to know the maximum possible value X_{max} of the tensor batch. Since different color models have different X_{max} , this value must be predefined according to the selected color model. Once X_{max} is defined, n_{bit} can be calculate as $\lceil \log_2(X_{max}) \rceil$.

To calculate the bit planes of an unnormalized integer input tensor batch X , we perform element-wise division of X by 2. The remainder from this division constitutes a bit plane of X , while the quotient is saved for the extraction of subsequent bit planes. This process is repeated until we obtain n_{bit} bit planes.

The resulting bit planes are then concatenated to form n_{bit} binary tensor batch of X_{shape} . This format closely resembles that of rate coding and ensures determinism in the coding results without having to sample more than n_{bit} times.

Symbol	Meaning
X	Input image tensors
X_{max}	Integer value indicate the maximum value of input image tensor
n_{bit}	Minimum number of bit planes required to encode input X into bit planes
$\log_2()$	Binary logarithm function
X_{shape}	Dimensions of X, usually include number of images being processed B , number of channels C and resolution H, W
$concat()$	Tensor concatenation function, concatenating a list of tensors resulted to a tensor contain spikes of shape (n_{bit}, X_{shape})
L	A list-like [41] data structure, used to temporarily store coding result
\mathbb{Z}	The set of all integers

TABLE II: Table of symbols used in Algorithm 1.

Algorithm 1 Bit plane coding algorithm

Require: X_{max} is defined, $X_{max} > 0$ and $X \in \mathbb{Z}$

function BITPLANEENCODE(X, X_{max})

$n_{bit} \leftarrow \lceil \log_2(X_{max}) \rceil$ ▷ Get number of bit required to encode image from highest possible value X

$L \leftarrow []$ ▷ Empty list initialization

for each $X_{shape}.C$ **do**

for $i \leftarrow 0, i < n_{bit}, i++$ **do**

$L.insert(X \bmod 2)$ ▷ Element-wise modulo of tensor, then store the bit plane to L

$X \leftarrow \lfloor X/2 \rfloor$ ▷ Element-wise division of input image tensor and floor the result

end for

end for

return $concat(L)$ ▷ Concatenate all stored sub tensors in L to a single tensor

end function

V. EXPERIMENTS

A. Experimental settings

To investigate performance of SNN for images, we employed the popular tool SEW-ResNet18 with ADD element-wise function [25]. The model and experiment process were implemented using PyTorch [42] and SpikingJelly [43]. Color conversion algorithms are based on implementations from Kornia [44]. For the baseline method in the experiments, the spike rate coding is employed with a step size of 10. To facilitate optimization, we utilize surrogate gradient methods applied to all IF neurons using the arctan surrogate function $S(U)$ [13], [25] with the defined derivative ∂S of:

$$\frac{\partial S}{\partial U} = \frac{1}{\pi} \cdot \frac{1}{1 + (\pi U)^2} \quad (7)$$

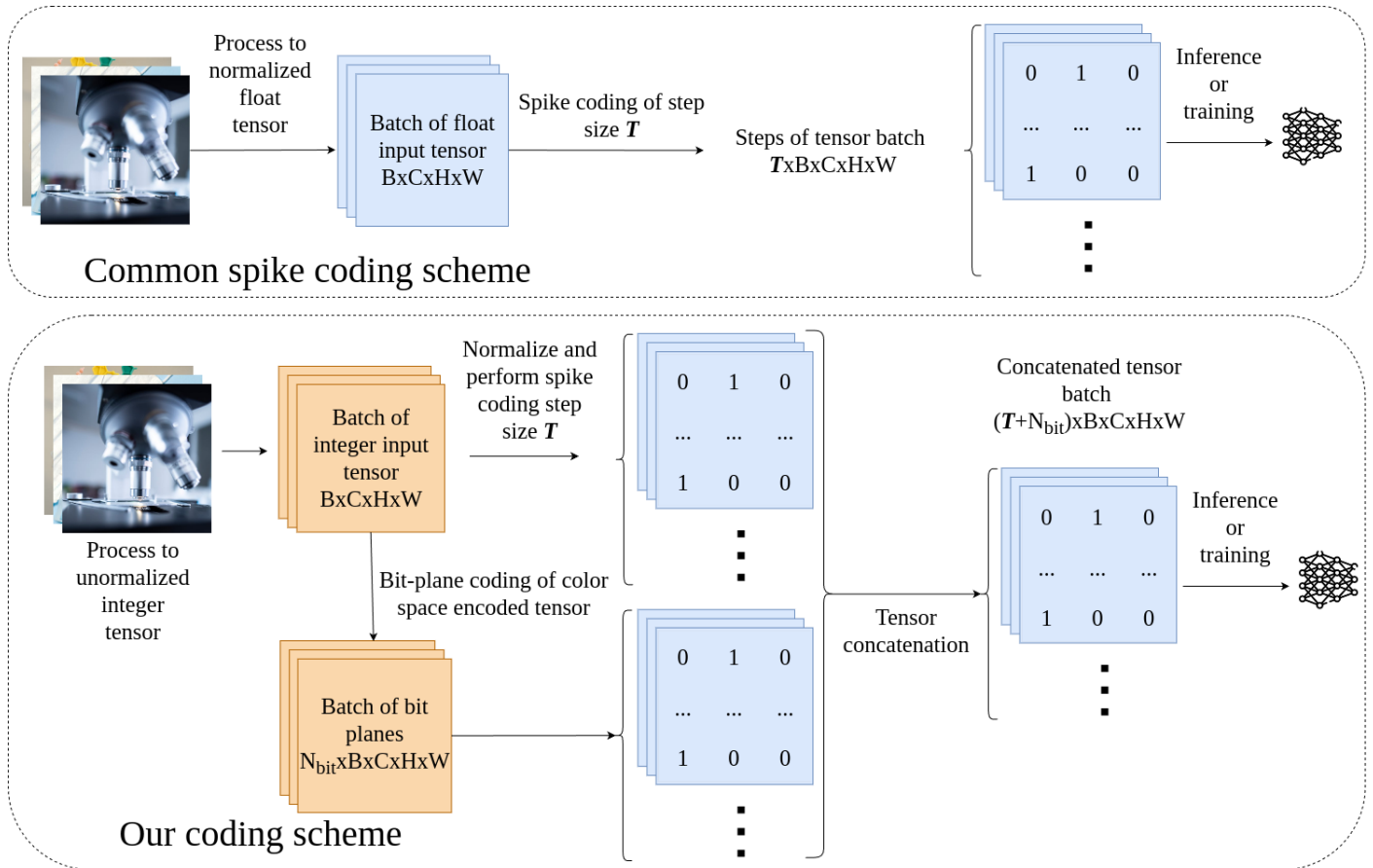


Fig. 2: Our proposed coding method (lower) compare with traditional spike coding method (upper).

The optimization process is conducted with the Adam algorithm [45], using a learning rate of $lr = 1 \times 10^{-3}$ and parameters $\beta = (0.9, 0.999)$ across all evaluated datasets. Cross-Entropy Loss with Softmax function and mean reduction $L(x, y)$ [42] across N mini-batch dimension was also widely employed as the loss function:

$$L(x, y) = \frac{\sum_{n=1}^N l_n}{N}, \quad (8)$$

$$l_n = - \sum_{c=1}^C w_c \log \frac{\exp\{x_{n,c}\}}{\sum_{i=1}^C \exp\{x_{n,i}\}} y_{n,c}$$

where l_n is loss of each mini-batch, x is the input, y is the target, w is the weight, C is the total amount of class where $i \in C$ and c is the mini-classes.

In the first part of our experiments, we only use grayscale image datasets to clearly see the effects of bit plane coding. In the second part, popular datasets of color images are used to see the practical effects of both bit plane coding and color models. We allocated 80% of each dataset for training and the remaining 20% with deterministic random seeding for validation. All datasets were processed with a batch size of 16 images for 100 epochs on an NVIDIA RTX 3090 GPU.

B. Experimental Results

In this part, we will discuss results of our main experiments along with some interesting findings beside original hypotheses.

Dataset	Accuracy of coding methods (%)		
	Baseline	Bit plane coding only	Proposed method
MNIST [36]	98.62	97.87	98.93
KMNIST [46]	94.13	92.33	95.58
Fashion-MNIST [47]	88.83	86.66	90.19

TABLE III: Comparison of validation accuracy among three coding methods. Best value is highlighted in bold.

1) The effect of bit plane coding on grayscale images:

First, we aim to investigate whether the proposed approach yields any significant or insightful results without impacts of color information. For that, we employed three popular datasets of grayscale images, including MNIST [36], KMNIST [46], Fashion-MNIST [47]. The results of MNIST dataset were already shown in Table I. However, they are still included here to see the behaviors of the coding methods over different datasets. As grayscale images consist of only intensity values

Dataset	Analysis results of coding methods (bits)					
	Baseline		Bit plane coding only		Proposed method	
	AKC	SE	AKC	SE	AKC	SE
MNIST [36]	721.5	0.53	772.8	0.56	744.4	0.55
KMNIST [46]	1093	0.70	1221	0.70	1150	0.70
Fashion-MNIST [47]	1384	0.86	1377	0.82	1381	0.84

TABLE IV: Comparison of analysis results among coding methods, contains the approximated Kolmogorov complexity (abbreviated AKC) and Shannon Entropy (abbreviated SE). Highest values of AKC are denoted in red and lowest are denoted in blue.

ranging between [0, 255], we apply our coding process with one channel. This process would produce eight bit-plane channels that represent the image information in binary form. In this part, we investigate three options, namely 1) the baseline model (spike coding only), 2) using bit plane coding only, 3) the proposed model (spike coding combined with bit plane coding).

As demonstrated in Table III, the combination of spike coding with bit-plane coding outperformed other coding methods in terms of validation accuracy. As mentioned, using only bit-plane coding resulted in a reduction in accuracy; however, the combination of spike coding with bit plane coding (i.e. the proposed method) provides gain in all datasets. For any method, the accuracy value is highest with the MNIST dataset and lowest with the Fashion-MNIST dataset. This could be because among these three datasets, MNIST is the simplest one while Fashion-MNIST is the most complex one. Interestingly, the gain of the proposed method compared to the baseline is increased from 0.31% (with MNIST) to roughly 1.4% (with KMNIST and Fashion-MNIST). That means the impact of bit plane coding is more prominent with more complex datasets.

Upon further analysis of spike distribution complexities for various coding methods, as presented in Table IV, several insights emerge.

First, we observe that the baseline method has the lowest complexity in MNIST and KMNIST datasets, while it has the highest complexity in the Fashion-MNIST dataset. We suspect that this difference stems from the nature of these datasets. Both MNIST and KMNIST primarily use binary pixel values, with zeros representing the background and ones indicating the presence of a character. This binary representation results in a simpler spike distribution. In contrast, Fashion-MNIST employs a wider range of pixel values to capture the textures of various clothing items, which introduces greater complexity into the spike distribution when using baseline coding methods. This observation suggests that more complex visual datasets may lead to even more pronounced differences in spike distribution when using these coding methods.

Additionally, by introducing a hybrid coding approach that combines baseline and bit plane coding methods, we hypothe-

size the potential existence of an optimal complexity threshold at which the SNN might achieve peak performance. This idea of an optimizable global maximum suggests that complexity thresholds could play a key role in determining SNN effectiveness. Based on our data, we propose that measuring spike distribution complexity could be crucial in tuning SNNs to perform optimally across different datasets and tasks.

Dataset	Accuracy of coding methods (%)		
	Baseline	Bit plane coding only	Proposed method
CIFAR10 [26]	70.69	37.28	73.49
CIFAR100 [26]	38.57	11.28	42.15
Caltech101 [48]	61.67	43.28	64.55
Caltech256 [49]	30.04	21.75	41.51
EuroSAT [50]	84.39	79.87	88.48
Imagenette [51]	72.99	48.20	78.68
Food101 [52]	19.62	6.29	36.95
GTSRB [53]	93.36	95.85	95.35

TABLE V: Average validation accuracy on various computer vision dataset of our proposed method.

Dataset	Analysis results of coding methods (bits)					
	Baseline		Bit plane coding only		Proposed method	
	AKC	SE	AKC	SE	AKC	SE
CIFAR10 [26]	7530	0.995	6764	0.996	7190	0.995
CIFAR100 [26]	7374	0.995	6710	0.996	7079	0.995
Caltech101 [48]	310k	0.993	260k	0.992	279k	0.992
Caltech256 [49]	307k	0.991	257k	0.990	276k	0.990
EuroSAT [50]	30.3k	0.953	22.9k	0.944	27.0k	0.949
Imagenette [51]	334k	0.987	282k	0.994	302k	0.992
Food101 [52]	339k	0.989	288k	0.995	308k	0.993
GTSRB [53]	308k	0.902	2914	0.223	5791	0.019

TABLE VI: Comparison of analysis results among coding methods, contains the approximated Kolmogorov complexity (abbreviated AKC) and Shannon Entropy (abbreviated SE), values in thousands are represented with *k* (e.g., 22k = 22,000). Highest values of AKC are denoted in red and lowest are denoted in blue.

2) *The effect of bit plane coding on color images:* For our experiment, we conducted tests on various color-image classification datasets, including CIFAR10 [26], CIFAR100 [26], EuroSAT [50], Caltech101 [48], Caltech256 [49], Imagenette [51] (which is a subset of ImageNet [54]), GTSRB [53], and Food101 [52]. The default color model of these datasets is RGB. Due to computing resource constraints of the simulation tool, large images are downsampled to 224x224 pixels. So, among these datasets, CIFAR10 [26], CIFAR100 [26] and EuroSAT [50] are trained with original input size while images of all other dataset are resized to 224x224 pixels.

Across all tested datasets, our proposed methods consistently outperform the baseline method, with the notable exception of the GTSRB [53] dataset, where bit-plane coding alone appears to yield the best performance without the need for combination with traditional spike coding. This observation

Dataset	Analysis results of coding methods (bits)													
	With RGB encoded (Ours)		With CMY encoded (Ours)		With YCbCr encoded (Ours)		With HSL encoded (Ours)		With HSV encoded (Ours)		With CIE XYZ encoded (Ours)		With CIE LAB encoded (Ours)	
	AKC	SE	AKC	SE	AKC	SE	AKC	SE	AKC	SE	AKC	SE	AKC	SE
CIFAR10 [26]	7190	0.995	7086	0.992	6671	0.972	6634	0.927	6752	0.957	7083	0.986	6857	0.988
CIFAR100 [26]	7079	0.995	6975	0.991	6606	0.974	6551	0.929	6660	0.955	6984	0.987	6769	0.985
Caltech101 [48]	279k	0.992	269k	0.978	231k	0.957	241k	0.905	242k	0.929	268k	0.989	239k	0.971
Caltech256 [49]	276k	0.990	265k	0.976	233k	0.957	243k	0.907	244k	0.933	244k	0.989	242k	0.972
EuroSAT [50]	27.0k	0.949	26.5k	0.968	25.2k	0.944	25.3k	0.993	25.8k	0.950	26.2k	0.932	25.9k	0.966
Imagenette [51]	302k	0.992	292k	0.989	267k	0.957	271k	0.901	276k	0.941	288k	0.979	277k	0.976
Food101 [52]	308k	0.993	297k	0.990	273k	0.986	277k	0.908	280k	0.927	294k	0.975	281k	0.969
GTSRB [53]	5791	0.019	5706	0.006	17.6k	0.489	86.1k	0.462	92.9k	0.499	5704	0.005	5703	0.006

TABLE VII: Comparison of analysis results with our proposed coding method across all tested color models, contains the approximated Kolmogorov complexity (abbreviated AKC) and Shannon Entropy (abbreviated SE) measured in bits, values in thousands are represented with k (e.g., 22k = 22,000). Highest values of AKC are denoted in red and lowest are denoted in blue.

Dataset	Accuracy of coding methods (%)							
	With RGB encoded (Ours)	With CMY encoded (Ours)	With YCbCr encoded (Ours)	With HSL encoded (Ours)	With HSV encoded (Ours)	With CIE XYZ encoded (Ours)	With CIE LAB encoded (Ours)	
CIFAR10 [26]	73.49	73.73	73.64	73.39	73.06	73.63	74.06	
CIFAR100 [26]	42.15	41.31	41.62	41.94	41.91	41.73	42.03	
Caltech101 [48]	64.55	65.65	65.53	66.46	68.41	65.30	66.22	
Caltech256 [49]	41.51	40.65	40.84	40.55	39.94	40.50	40.79	
EuroSAT [50]	88.48	86.61	88.11	88.74	88.81	88.87	87.48	
Imagenette [51]	78.68	77.35	78.78	78.55	78.50	77.35	78.70	
Food101 [52]	36.95	37.71	36.98	38.03	36.41	37.10	35.87	
GTSRB [53]	95.35	51.36	70.68	79.18	80.86	51.78	51.78	
Average	65.15	59.21	62.02	63.36	63.49	59.53	59.61	

TABLE VIII: Comparison of validation accuracy among coding methods.

suggests that while our methods generally enhance performance by improving the representation of spike distributions, certain datasets may favor different coding approaches depending on their visual complexity and specific characteristics. In the GTSRB [53] case, it seems that bit-plane coding alone is sufficient to capture the essential features for effective processing.

The analysis results presented in Table VI highlight the relationship between complexity and performance in different coding methods. Bit-plane coding consistently exhibits lower complexities across datasets, while traditional spike coding tends to produce higher complexity values. This outcome aligns with our hypothesis that complexity increases in visual datasets with greater detail and variation.

In further investigating the GTSRB [53] dataset, we observed a significant reduction in spike distribution complexity (over 99% when comparing baseline with proposed scheme and pure bit planes coding in Table VI) alongside improved model performance. Usually a decrease in complexity can sometimes indicate a loss of critical information, it may also suggest that the spike distribution has become more streamlined, capturing essential features more effectively. However, a complexity reduction at such large scale could also introduce elements of instability (shown in Table VII), as it can be challenging to discern whether the decreased complexity represents a beneficial simplification or a detrimental loss of

information.

Consequently, while our findings indicate promising results, we suggest further exploration of complexity thresholds to ensure consistent performance across varying datasets.

3) *Impacts of color models*: In this part, also we investigate two options, namely 1) the baseline method and 2) proposed method.

The accuracy results of different cases are shown in Table VIII. We can see that, when using RGB color model, the accuracy of the proposed method is always higher than that of the baseline. The gain ranges from about 2% (with GTSRB [53] dataset) up to 11% (with Caltech256 [49] dataset), depending on the employed dataset. This suggests that the benefit of the proposed method when applying to color images is more significant than when applying to grayscale images.

Interestingly, the results show that RGB is not always the best color model. Among the eight datasets, RGB provides the best performance in three cases (namely CIFAR100 [26], Caltech256 [49], GTSRB [53]). CMY does not achieve any best results, whereas each of the other five color models achieves the best performance once. Especially, with Caltech101 [48] dataset, the accuracy of HSV color model is 68.41%, which is much higher than that of RGB color model (64.55%).

When considering the average of accuracy values across all datasets, the RGB color model is significantly better than other color models (mentioned the last row of Table VIII) and

even though there are performance degradation on GTSRB [53], averaged result across all dataset proven to at least outperformed baseline method.

From the above discussion, the key findings of our research can be summarized as follows.

- The proposed method provides benefits for both grayscale images and color images.
- The gain of the proposed method depends on the employed dataset. For practical color datasets, the gain is from 2% up to 11%.
- In terms of average accuracy value over all datasets, RGB is the best color model and CMY is the worst one.
- However, considering individual datasets, RGB is not always the best color model. It provides the best performance in only three datasets.
- Especially, with the Caltech101 dataset, the performance of HSV color model (68.41%) is much better than that of the RGB color model (64.55%).

VI. DISCUSSION

A. Complexity or entropy?

In this study, we employ two primary metrics, an approximated Kolmogorov complexity and Shannon entropy, to analyze the effects of bit-plane coding on the distribution of spike trains. These metrics were chosen because they are widely used in signal processing and information theory, making them well-suited for analyzing the coded spike and bit-plane signals. By treating both coded spikes and bit planes as types of signals, we believe that Kolmogorov complexity and Shannon entropy can provide valuable insights into the complexity of spike distributions. While we conducted limited analysis with Shannon entropy, our results indicate a positive correlation between Shannon entropy and Kolmogorov complexity. This suggests that Shannon entropy could serve as an alternative to Kolmogorov complexity for those interested in measurement and analysis. However, we find Kolmogorov complexity to be more effective, as it provides clearer distinctions between measurements when compared to Shannon entropy.

Despite achieving substantial insights through these metrics, we recognize that measuring complexity and entropy alone may not fully capture the intricacies of image data. Images inherently contain structural complexity and spatial information, which can be difficult to quantify and analyze. Focusing solely on spike signals as sequential data may overlook these aspects. A helpful analogy is the historical debate in physics regarding the nature of light, with some scientists viewing light as a wave and others as particles. It was only with the discovery of wave-particle duality through experiments like the double-slit experiment that a more comprehensive understanding emerged. Similarly, viewing spike signals solely as sequential signals could reveal certain patterns but may not capture the full complexity underlying the optimization process in image processing tasks. Currently, tools designed

specifically for spike signal analysis that incorporate spatial information for image-based tasks are underexplored. This gap highlights the need for further research into analysis methods that can integrate both signal and spatial information for more complete insights.

VII. CONCLUSION

In conclusion, our research introduces a novel coding method for SNN that leverages bit planes derived from various color models of input image data. This approach prove to enhances the computational accuracy of SNN without increasing the model size. Through extensive experimental validation, we have demonstrated the effectiveness of our coding strategy across multiple computer vision tasks, achieving notable performance gains compared to conventional methods. This study is pioneering in its application of color models within the context of spiking neural networks, and we believe that our findings open new avenues for the development of more efficient and effective SNN models. Our work sets a foundation for future research and applications, potentially advancing the field of computational neuroscience and artificial intelligence.

REFERENCES

- [1] M. A. Wani, F. A. Bhat, S. Afzal, and A. I. Khan, *Advances in deep learning*. Springer, 2020.
- [2] D.-A. Nguyen, X.-T. Tran, and F. Iacopi, "A review of algorithms and hardware implementations for spiking neural networks," *Journal of Low Power Electronics and Applications*, vol. 11, no. 2, p. 23, 2021.
- [3] D. Auge, J. Hille, E. Mueller, and A. Knoll, "A survey of encoding techniques for signal processing in spiking neural networks," *Neural Processing Letters*, vol. 53, no. 6, pp. 4693–4710, 2021.
- [4] P. Blouw, X. Choo, E. Hunsberger, and C. Eliasmith, "Benchmarking keyword spotting efficiency on neuromorphic hardware," in *Proceedings of the 7th annual neuro-inspired computational elements workshop*, 2019, pp. 1–8.
- [5] B. Rajendran, A. Sebastian, M. Schmuker, N. Srinivasa, and E. Eleftheriou, "Low-power neuromorphic hardware for signal processing applications: A review of architectural and system-level design approaches," *IEEE Signal Processing Magazine*, vol. 36, no. 6, pp. 97–110, 2019.
- [6] J. D. Nunes, M. Carvalho, D. Carneiro, and J. S. Cardoso, "Spiking neural networks: A survey," *IEEE Access*, vol. 10, pp. 60 738–60 764, 2022.
- [7] G. Srinivasan, S. Roy, V. Raghunathan, and K. Roy, "Spike timing dependent plasticity based enhanced self-learning for efficient pattern recognition in spiking neural networks," in *2017 International Joint Conference on Neural Networks (IJCNN)*. IEEE, 2017, pp. 1847–1854.
- [8] F. Liu, W. Zhao, Y. Chen, Z. Wang, T. Yang, and L. Jiang, "Sstdp: Supervised spike timing dependent plasticity for efficient spiking neural network training," *Frontiers in Neuroscience*, vol. 15, p. 756876, 2021.
- [9] E. O. Neftci, H. Mostafa, and F. Zenke, "Surrogate gradient learning in spiking neural networks: Bringing the power of gradient-based optimization to spiking neural networks," *IEEE Signal Processing Magazine*, vol. 36, no. 6, pp. 51–63, 2019.
- [10] L. Vorabbi, D. Maltoni, and S. Santi, "Input layer binarization with bit-plane encoding," in *International Conference on Artificial Neural Networks*. Springer, 2023, pp. 395–406.
- [11] S. N. Gowda and C. Yuan, "Colomet: Investigating the importance of color spaces for image classification," in *Computer Vision—ACCV 2018: 14th Asian Conference on Computer Vision, Perth, Australia, December 2–6, 2018, Revised Selected Papers, Part IV 14*. Springer, 2019, pp. 581–596.

- [12] J. Taipalmaa, N. Passalis, and J. Raitoharju, "Different color spaces in deep learning-based water segmentation for autonomous marine operations," in *2020 IEEE international conference on image processing (ICIP)*. IEEE, 2020, pp. 3169–3173.
- [13] J. K. Eshraghian, M. Ward, E. O. Nefci, X. Wang, G. Lenz, G. Dwivedi, M. Bennamoun, D. S. Jeong, and W. D. Lu, "Training spiking neural networks using lessons from deep learning," *Proceedings of the IEEE*, 2023.
- [14] N. Luu, D. Luu, P. N. Nam, and T. C. Thang, "Improvement of spiking neural network with bit plane coding," in *2024 IEEE 16th International Conference on Computational Intelligence and Communication Networks (CICN)*. IEEE, 2024.
- [15] S. Ghosh-Dastidar and H. Adeli, "Spiking neural networks," *International journal of neural systems*, vol. 19, no. 04, pp. 295–308, 2009.
- [16] W. Maass, "Networks of spiking neurons: the third generation of neural network models," *Neural networks*, vol. 10, no. 9, pp. 1659–1671, 1997.
- [17] N. C. Thompson, K. Greenewald, K. Lee, and G. F. Manso, "The computational limits of deep learning," *arXiv preprint arXiv:2007.05558*, vol. 10, 2020.
- [18] I. Goodfellow, Y. Bengio, and A. Courville, *Deep learning*. MIT press, 2016.
- [19] T. J. Sejnowski, C. Koch, and P. S. Churchland, "Computational neuroscience," *Science*, vol. 241, no. 4871, pp. 1299–1306, 1988.
- [20] A. Zjajo, J. Hofmann, G. J. Christiaanse, M. Van Eijk, G. Smaragdos, C. Strydis, A. De Graaf, C. Galuzzi, and R. Van Leuken, "A real-time reconfigurable multichip architecture for large-scale biophysically accurate neuron simulation," *IEEE transactions on biomedical circuits and systems*, vol. 12, no. 2, pp. 326–337, 2018.
- [21] W. Gerstner, "Spike-response model," *Scholarpedia*, vol. 3, no. 12, p. 1343, 2008.
- [22] L. F. Abbott, "Lapicque's introduction of the integrate-and-fire model neuron (1907)," *Brain research bulletin*, vol. 50, no. 5-6, pp. 303–304, 1999.
- [23] P. U. Diehl, D. Neil, J. Binas, M. Cook, S.-C. Liu, and M. Pfeiffer, "Fast-classifying, high-accuracy spiking deep networks through weight and threshold balancing," in *2015 International joint conference on neural networks (IJCNN)*. IEEE, 2015, pp. 1–8.
- [24] L. Zhang, S. Zhou, T. Zhi, Z. Du, and Y. Chen, "Tdsnn: From deep neural networks to deep spike neural networks with temporal-coding," in *Proceedings of the AAAI conference on artificial intelligence*, vol. 33, no. 01, 2019, pp. 1319–1326.
- [25] W. Fang, Z. Yu, Y. Chen, T. Huang, T. Masquelier, and Y. Tian, "Deep residual learning in spiking neural networks," *Advances in Neural Information Processing Systems*, vol. 34, pp. 21 056–21 069, 2021.
- [26] K. Alex, "Learning multiple layers of features from tiny images," <https://www.cs.toronto.edu/kriz/learning-features-2009-TR.pdf>, 2009.
- [27] K. He, X. Zhang, S. Ren, and J. Sun, "Deep residual learning for image recognition," in *Proceedings of the IEEE conference on computer vision and pattern recognition*, 2016, pp. 770–778.
- [28] Y. Hu, H. Tang, and G. Pan, "Spiking deep residual networks," *IEEE Transactions on Neural Networks and Learning Systems*, vol. 34, no. 8, pp. 5200–5205, 2021.
- [29] D. Huh and T. J. Sejnowski, "Gradient descent for spiking neural networks," *Advances in neural information processing systems*, vol. 31, 2018.
- [30] Y. Liu, J. Dong, and P. Zhou, "Defending against adversarial attacks in deep learning with robust auxiliary classifiers utilizing bit-plane slicing," *ACM Journal on Emerging Technologies in Computing Systems (JETC)*, vol. 18, no. 3, pp. 1–17, 2022.
- [31] G. Chen, Y. Chen, Z. Yuan, X. Lu, X. Zhu, and W. Li, "Breast cancer image classification based on cnn and bit-plane slicing," in *2019 International Conference on Medical Imaging Physics and Engineering (ICMIPE)*. IEEE, 2019, pp. 1–4.
- [32] N. A. Ibraheem, M. M. Hasan, R. Z. Khan, and P. K. Mishra, "Understanding color models: a review," *ARPJ Journal of science and technology*, vol. 2, no. 3, pp. 265–275, 2012.
- [33] K. N. Plataniotis, "Color image processing and applications," *Measurement Science and Technology*, vol. 12, no. 2, pp. 222–222, 2001.
- [34] H.-K. Kim, J. H. Park, and H.-Y. Jung, "An efficient color space for deep-learning based traffic light recognition," *Journal of Advanced Transportation*, vol. 2018, no. 1, p. 2365414, 2018.
- [35] M. Chyad, B. Zaidan, A. Zaidan, H. Pilehkouhi, R. Aalaa, S. Qahtan, H. A. Alsattar, D. Pamucar, and V. Simic, "Exploring adversarial deep learning for fusion in multi-color channel skin detection applications," *Information Fusion*, vol. 114, p. 102632, 2025.
- [36] L. Deng, "The mnist database of handwritten digit images for machine learning research [best of the web]," *IEEE signal processing magazine*, vol. 29, no. 6, pp. 141–142, 2012.
- [37] C. E. Shannon, "A mathematical theory of communication," *The Bell system technical journal*, vol. 27, no. 3, pp. 379–423, 1948.
- [38] P. Deutsch, "Deflate compressed data format specification version 1.3," Tech. Rep., 1996.
- [39] D. A. Huffman, "A method for the construction of minimum-redundancy codes," *Proceedings of the IRE*, vol. 40, no. 9, pp. 1098–1101, 1952.
- [40] J. Ziv and A. Lempel, "A universal algorithm for sequential data compression," *IEEE Transactions on information theory*, vol. 23, no. 3, pp. 337–343, 1977.
- [41] H. Abelson and G. J. Sussman, *Structure and interpretation of computer programs*. The MIT Press, 1996.
- [42] A. Paszke, S. Gross, F. Massa, A. Lerer, J. Bradbury, G. Chanan, T. Killeen, Z. Lin, N. Gimelshein, L. Antiga *et al.*, "Pytorch: An imperative style, high-performance deep learning library," *Advances in neural information processing systems*, vol. 32, 2019.
- [43] W. Fang, Y. Chen, J. Ding, Z. Yu, T. Masquelier, D. Chen, L. Huang, H. Zhou, G. Li, and Y. Tian, "Spikingjelly: An open-source machine learning infrastructure platform for spike-based intelligence," *Science Advances*, vol. 9, no. 40, p. eadi1480, 2023. [Online]. Available: <https://www.science.org/doi/abs/10.1126/sciadv.adi1480>
- [44] E. Riba, D. Mishkin, D. Ponsa, E. Rublee, and G. Bradski, "Kornia: an open source differentiable computer vision library for pytorch," in *Winter Conference on Applications of Computer Vision*, 2020. [Online]. Available: <https://arxiv.org/pdf/1910.02190.pdf>
- [45] D. P. Kingma and J. Ba, "Adam: A method for stochastic optimization," *arXiv preprint arXiv:1412.6980*, 2014.
- [46] T. Clanuwat, M. Bober-Irizar, A. Kitamoto, A. Lamb, K. Yamamoto, and D. Ha. (2018) Deep learning for classical japanese literature.
- [47] H. Xiao, K. Rasul, and R. Vollgraf, "Fashion-mnist: a novel image dataset for benchmarking machine learning algorithms," *arXiv preprint arXiv:1708.07747*, 2017.
- [48] F.-F. Li, M. Andreeto, M. Ranzato, and P. Perona, "Caltech 101," Apr 2022.
- [49] G. Griffin, A. Holub, and P. Perona, "Caltech 256," Apr 2022.
- [50] P. Helber, B. Bischke, A. Dengel, and D. Borth, "Eurosat: A novel dataset and deep learning benchmark for land use and land cover classification," *IEEE Journal of Selected Topics in Applied Earth Observations and Remote Sensing*, vol. 12, no. 7, pp. 2217–2226, 2019.
- [51] J. Howard, "Imagenette." [Online]. Available: <https://github.com/fastai/imagenette/>
- [52] L. Bossard, M. Guillaumin, and L. Van Gool, "Food-101 – mining discriminative components with random forests," in *European Conference on Computer Vision*, 2014.
- [53] J. Stallkamp, M. Schlipsing, J. Salmen, and C. Igel, "Man vs. computer: Benchmarking machine learning algorithms for traffic sign recognition," *Neural Networks*, no. 0, pp. –, 2012. [Online]. Available: <http://www.sciencedirect.com/science/article/pii/S0893608012000457>
- [54] J. Deng, W. Dong, R. Socher, L.-J. Li, K. Li, and L. Fei-Fei, "Imagenet: A large-scale hierarchical image database," in *2009 IEEE conference on computer vision and pattern recognition*. IEEE, 2009, pp. 248–255.
- [55] P. Umesh, "Image processing in python," *CSI Communications*, vol. 23, 2012.

APPENDIX A CMY OR CMYK?

In the initial stages of our experimental setup and algorithm design, we encountered challenges in selecting the appropriate device-dependent color model for our experiments. Specifically, we debated whether to use the CMY or CMYK color model. Each has advantages in different applications, but their compatibility with the neural networks used in our

research required careful consideration. In image processing and printing, the CMYK model was developed to improve print quality by reducing ink usage in darker regions. This is achieved by adding a K component, which reduces the CMY values proportionally, leading to enhanced contrast and more economical ink usage in printed images.

However, when adapting this approach for digital image processing, particularly for direct usage on digital devices, the inclusion of a K channel becomes less beneficial. Unlike printed images, digital displays do not require ink density adjustments, making the K channel unnecessary for accuracy. For our experiment, this would introduced dimensional conflicts in tested SNN architectures and coding schemes since they are previously optimized for three-channel data inputs (RGB), including a fourth channel would require additional modifications to model architecture, potentially affecting performance and comparability.

Furthermore, in our image processing pipeline, we observed that converting images to the CMYK color model using standard image processing libraries (e.g., PIL [55]) did not apply undercolor removal during conversion to CMYK model, resulting in a K channel of zero values. This posed a unique problem in our training setup: a zeroed K channel in the input data could nullify both the input signal and its gradients when surrogate gradients are used for backpropagation in SNNs. Consequently, this would undermine the learning process by reducing the effectiveness of gradient-based updates, complicating model training and ultimately impacting the accuracy of our results.

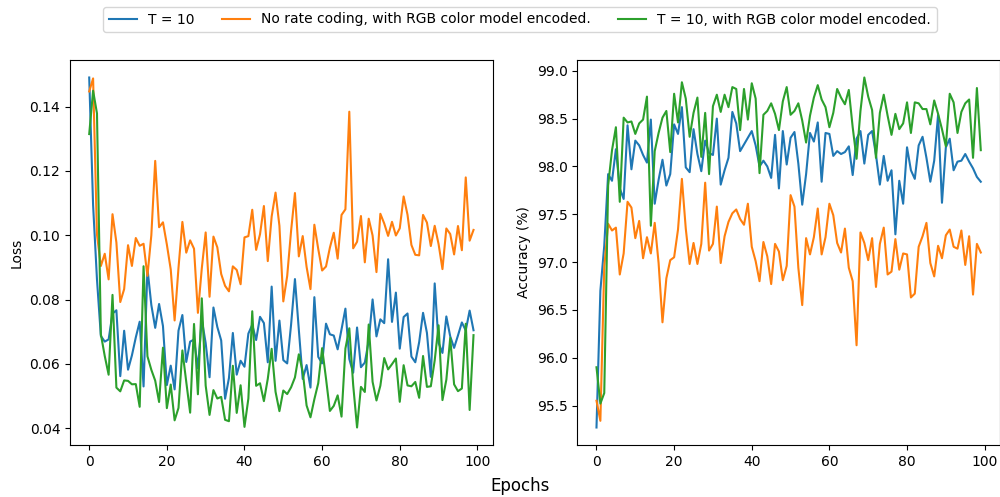
APPENDIX B

TRAINING PROGRESSION DETAILS

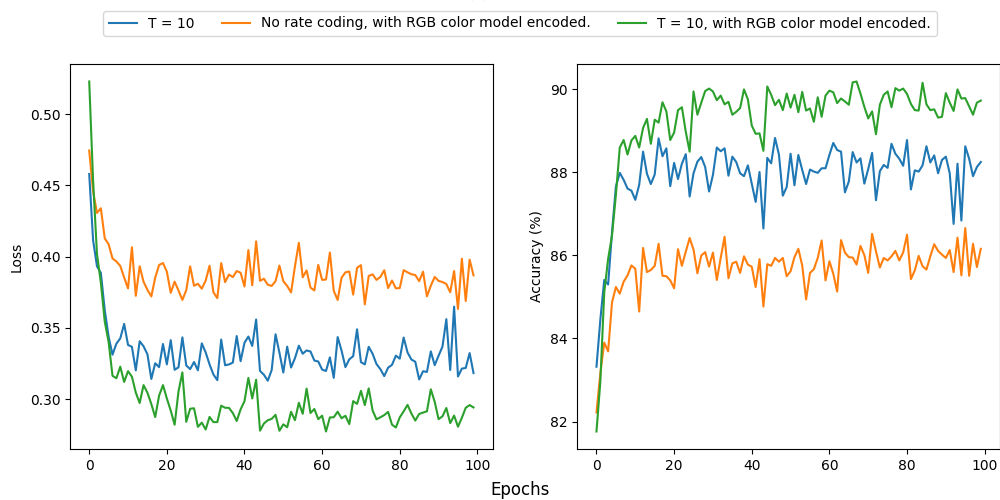
This section contain the training progression graph for each variant of experiments in Section V-B3 and Section V-B1.

It is noteworthy from Figure 4 and 5 that performance fluctuations were observed in both traditional coding and our coding method. We hypothesize that these fluctuations might related to inherent error rate during sampling process in Poisson-distributed spike trains [3].

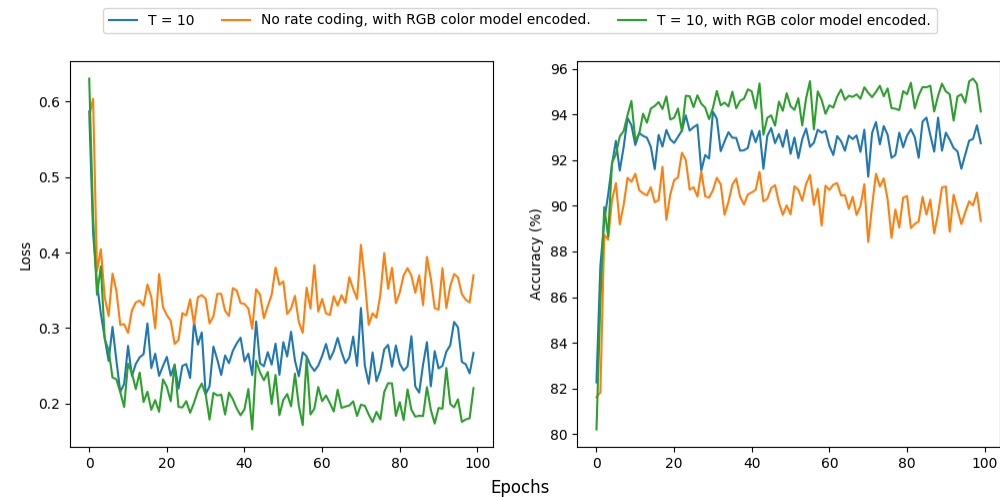
Another hypothesis is that although bit planes may possess a certain degree of spatial information, they can also encompass noise on low order bit planes that interferes with the training process or have little to none distinguishable features (which might explain how on low noises single-channel image dataset such as MNIST, the performance of only using bit planes coding remain competitive to traditional rate coding with less amount of time step). Consequently, the selective identification of bit planes that retain valuable spatial information continues to pose a significant challenge.



(a) MNIST



(b) Fashion-MNIST



(c) KMNIST

Fig. 3: Comparison in accuracy progression and loss progression between coding methods on different low-resolution gray-scale image classification datasets.

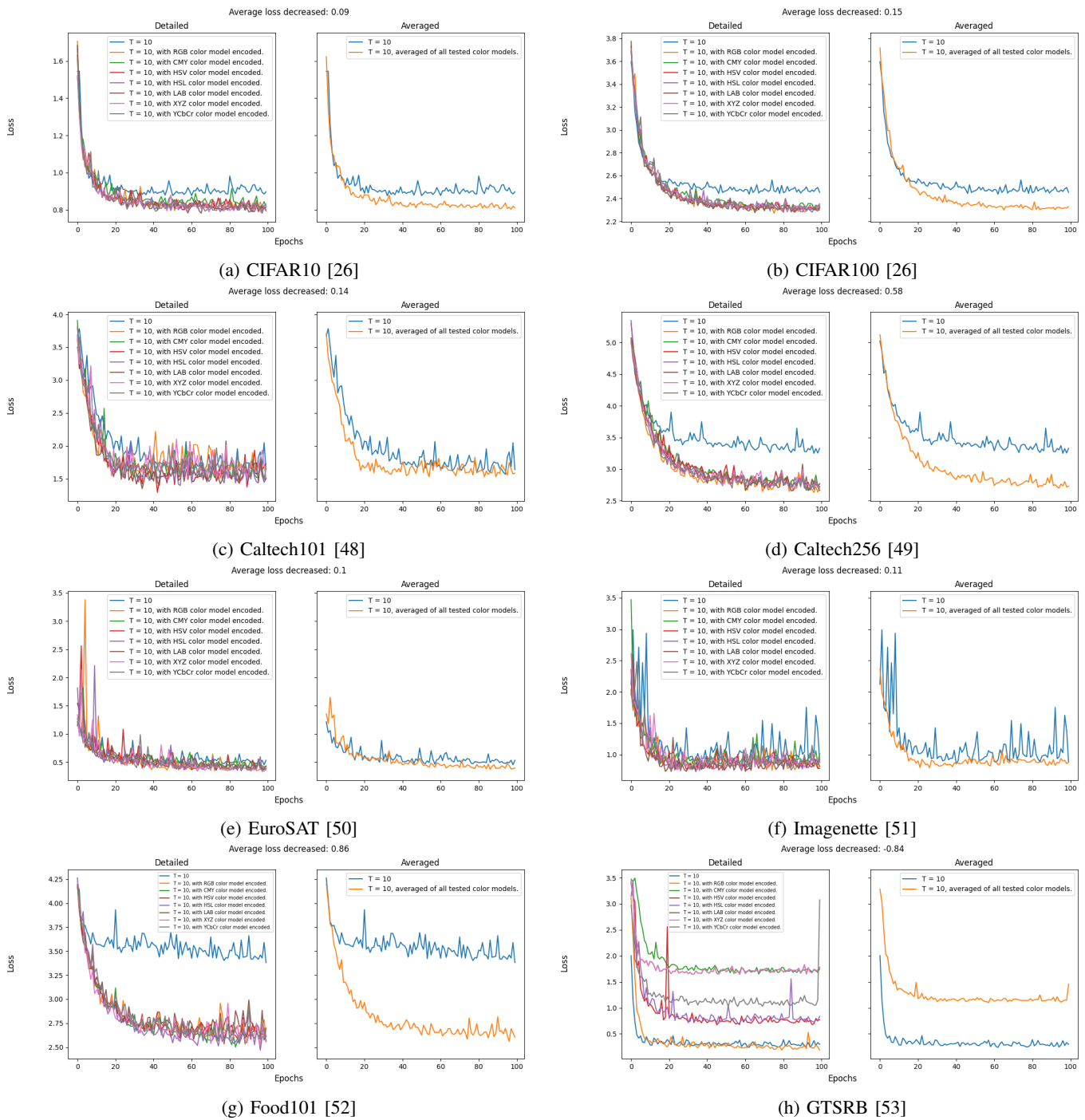
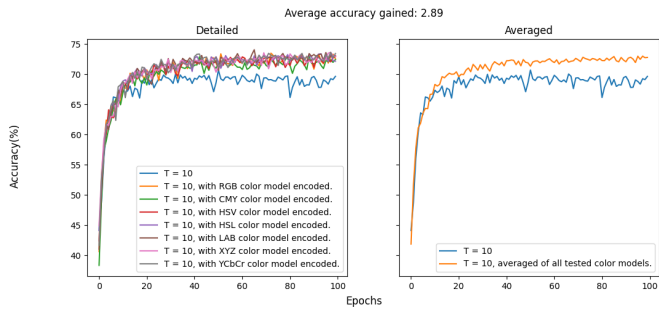
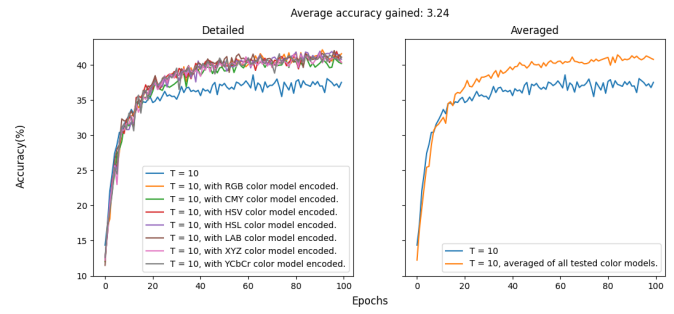


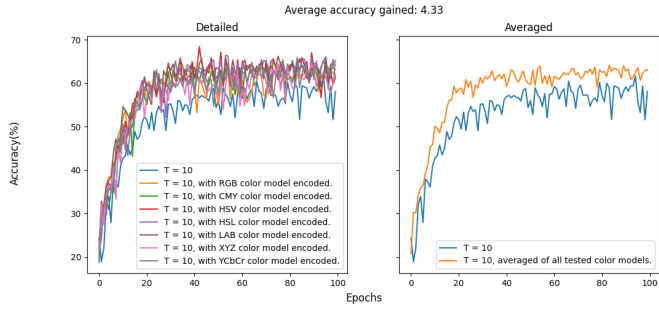
Fig. 4: Comparison in loss progression of traditional rate coding with our method on image classification datasets. On every sub-figure, loss details of every color models is shown on the left and average result of all models on the right with maximum loss difference denoted on top of figure.



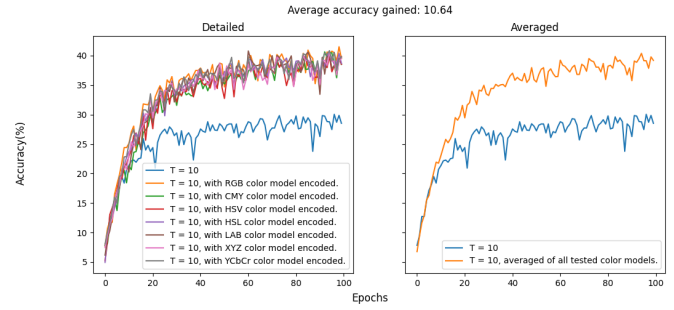
(a) CIFAR10 [26]



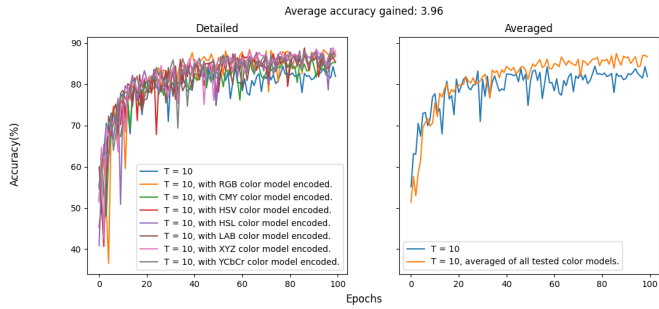
(b) CIFAR100 [26]



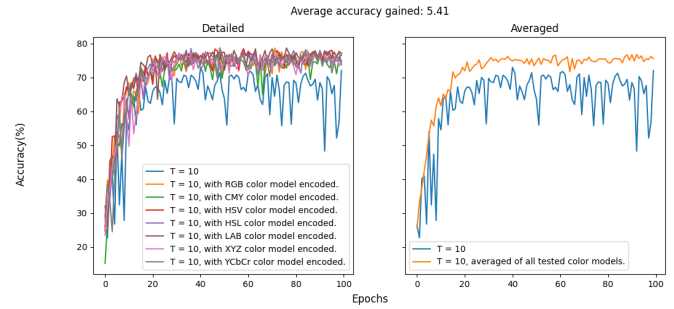
(c) Caltech101 [48]



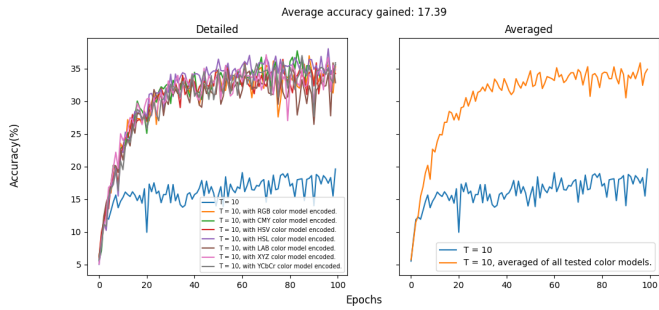
(d) Caltech256 [49]



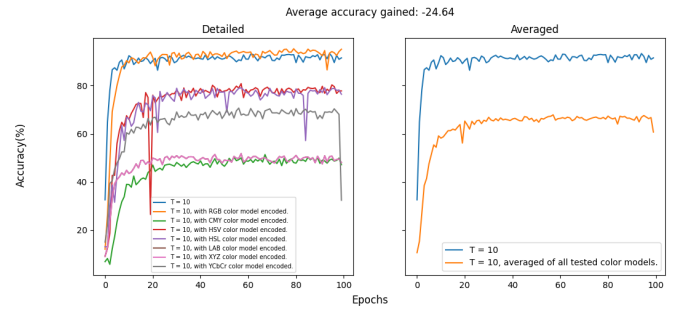
(e) EuroSAT [50]



(f) Imagenette [51]



(g) Food101 [52]



(h) GTSRB [53]

Fig. 5: Comparison in accuracy progression of traditional rate coding with our method on image classification datasets. On every sub-figure, accuracy details of every color models is shown on the left and average result of all models on the right with maximum accuracy difference denoted on top of figure.